SUNTEXT REVIEWS

SunText Review of Material Science

ISSN: 2766-5100

Open Access

Research Article

Volume 3:1

Effect of Heat Treatment on Dissimilar 316l And 316 Austenitic Stainless Steel TIG Welded Joints

Boumerzoug Z[1,*] and Delaunois F[2]

[1]LMSM, University of Biskra, B.P. 145, Biskra, Algeria

[2]Metallurgy Department, University of Mons, Belgium

[*]Corresponding author: Boumerzoug Z, LMSM, University of Biskra, B.P. 145, Biskra, Algeria; E-mail: z.boumerzoug@univ-biskra.dz

Received date: 03 September 2022; **Accepted date:** 07 September 2022; **Published date:** 09 September 2022

Citation: Boumerzoug Z, Delaunois F (2022). Effect of Heat Treatment on Dissimilar 316l And 316 Austenitic Stainless Steel TIG Welded Joints. SunText Rev Mat Sci 3(1): 116.

DOI: https://doi.org/10.51737/2766-5100.2022.016

Abstract

In this work, the effect of an isothermal heat treatment at 300°C on the evolution of the microstructure and the mechanical properties of welded dissimilar austenitic stainless steels 316L to 316 was studied by optical microscopy, scanning electron microscopy, analysis by energy dispersive spectroscopy, X-ray diffraction, and hardness measurements. It has been found that the fuzion zone is different from the heat affected zone and also from the base metal. A fusion line was observed in the welded joint. The heat treatments at 300°C had a particular mechanical and mechanical effect on the fusion zone.

Keywords: Austenitic stainless steel; Welding; Microstructures; Mechanical properties

Introduction

Based on the metallurgical microstructure classification, there are seven types of stainless steels: martensitic stainless steels, austenitic stainless steels, ferritic stainless steels, martensitic stainless steels, duplex stainless steels, precipitation hardening stainless steels and Mn-N substituted austenitic stainless steels [1]. Austenitic stainless steel is considered a first-class steel compared to other stainless steels due to the wide range of applications [2-4]. Austenitic stainless steel is a non-magnetic material, and is not intended to undergo hardening heat treatments [5]. Austenitic stainless steels have a face-centered cubic structure. In addition to their very high corrosion resistance, they are formable, easy to handle, which allows them to be used for a wide range of applications from high temperature to cryogenic temperature. The main alloying elements existing in these stainless steels are Cr and Ni. Cr has a dual role, it improves corrosion resistance and stabilizes the ferritic phase (called: ferrite stabilizer) [6]. The austenitic stainless steels that interest us in this study are the steels designated by 316 and 316L. 316 and 316L have excellent hot workability, weldability, toughness and resistance to pitting corrosion due to their high molybdenum content and austenitic microstructure. These steels perform well in several industries, such as the hydrocarbon industry and aerospace [7]. However, these two austenitic stainless steels have some key differences. 316L has a lower proportion of carbon in its composition and cannot exceed 0.03%, which decreases carbon precipitation, giving it good weldability and high corrosion resistance. On the other hand, 316 stainless steel has average carbon content and contains a proportion of molybdenum which varies between 2% and 3%, which increases its resistance to corrosion in an acid environment and at high temperature [8]. It is important to note that good weldability is one of the best characteristics of austenitic stainless steels. However, certain points interest researchers. During the welding of austenitic stainless steels, the problem of sensitization of the heat affected zone (HAZ) and hot cracking of the fusion zone remains a problem that should not be overlooked. Sensitization is the precipitation in the HAZ of carbides at grains boundaries, particularly chromium carbides. These carbides decrease the corrosion resistant properties of the metal. On the other hand, the cracks appear in the melting zone or the HAZ due to the weak melting of the metal compounds of sulfur and phosphorus [9]. Evaluated the mechanical properties of 316 L welds using tungsten inert gas welding. The microstructural study showed that the inclusions in the heat affected zone have a negative impact on the tensile strength of the weld joint [10]. Studied the effect of the number of passes on the microstructural and mechanical properties of submerged arc welding of 316L stainless steel. They found that as the number of passes increased, the tensile strength and hardness of the weld increased [11]. Singh et al. investigated the mechanical properties of gas tungsten arc welded 316L austenic stainless steels. They found the highest microhardness in Bbase metal (BM) compared to HAZ which was characterized by grain coarsening. Microscopic observation showed the dendritic structure in the fusion zone (FZ). In addition to this work, they investigated the effect of heat treatment on the welded joint. They also found that the extension of the aging time induces the precipitation of carbides and the coarsening of the grain size [12]. In this context, studied the effects of aging at temperatures between 550–850°C during 100 hours on the microstructure and mechanical properties of 316L austenitic stainless steel weld metal. They found that the dissolution of delta-ferrite and precipitation of the intermetallic sigma phase have an effect on the toughness and tensile of the welded joint [13]. Based on previous research, there are no studies dedicated to welding 316L stainless steel with 316 steel. However, there are studies that have been done on welding either of these two steels with other steels that belong to other classes of steels. The aim of the present work is to examine the effect of heat treatment at 300°C on the mechanisms of microstructure evolution and mechanical properties on the welded dissimilar stainless steels 316L to 316.

Experiment Procedure

Standart TIG welding process was made on tubular 316 and 316L austenitic stainless steels, using a filler wire ER316L. These stainless steels are used for oil installations. The chemical composition of the electode (ER316L) and the two dissimilar stainless steels (316 and 316L) are presented in (Table 1). To produce good quality welds a single V- butt joint with angle of 30° was prepared. The welding parameters were gas flow (Argon), voltage (20 V), welding speed (5 cm/min), current (100 A). Presents a macrographic view of the welded of tubular 316L to 316L austeitic stainless steel, which has been well made without any visual defects. In order to know the effect of heat treatments on the weld joint, an isothermal annealing at 300°C for 30 min was carried out in an electric furnace. This temperature is chosen in purpose, because in 316L stainless steel sensitization can be observed in the temperature ranging from 450°C to 900°C (Figure 1). Sensitization is a chromium carbide precipitation at grain boundaries which cause the occurrence of chromium-depleted zones at the grain boundaries. This sensitization phenomenon promotes the inter-granular corrosion. Microhardness measurements across the welded joint were performed using an INNOVATEST hardness tester with a load of 1000 g and a residence time of 15 s. For microstructural observations, the samples were polished with 120 to 2000 grade abrasive paper followed by a final polishing using a cloth containing a diamond pad with a grain size equal to 0.5 um. The revelation of the microstructure was carried out using a solution containing 30 ml of hydrochloric acid (HCl) and 10 ml of nitric acid (HNO3) and for 1m30s. The samples were analyzed by an optical microscope (HIROX Kh-8700) and a scanning electron microscope (HITACHI SU8020) equipped with an energy dispersive spectroscopy (EDS) detector. Phase analysis was performed by an analytical X-ray diffractometer (BRUKER D-5000) with cobalt radiation ($\lambda = 1.79$ Å).

Results and Discussion

Welded Joint

Shows a typical welded sample where it is possible to distinguish the fusion zone from the base metal and heat affected zone. The heat-affected zone is temporarily designated and it will be delimited by hardness measurements (Figure 2). Shows the microstructures taken from the different zones of the welded joint not heat-treated (Figure 3.a-e) and of the welded joint heat-treated at 300°C for 9 hours (Figure 3.a'-e'). First of all, for the welded and non-heat-treated joint, the microstructure of the fusion zone (3c and c') is totally different from either the heat-affected zone (3b, b', d and d') or the base metal (3a and a') (Figure 3). The microstructure of the fusion zone is similar to a solidification microstructure, as it is characterized by the formation of dendrites and elongated grains. The FZ is formed with two phases, austenic phase as matrix (dark color) and ferritic phase (δ) (white color). It has been reported by [14] that during the cooling process, the primary δ-ferrite solidifies in the melting zone and then transforms into austenite (γ). Since the $\delta \rightarrow \gamma$ transformation is a diffusion-controlled process, the rapid cooling in the TIG process does not provide enough time to complete the phase transformation. Therefore, part of the δ-ferrite is retained in FZ in dendritic "skeletal" form in the austenitic matrix. In addition, it is possible to observe a fusion line that separates the fusion zone and the HAZ. This fusion line will be discussed later. Concerning the HAZ, this zone is characterized by more or less large grains compared to the grains of the two base metals (316 or 316L). However, the effect of the heat treatment at 300 °C on the welded joint can be observed only on the fusion zone, contrary to the two other zones (HAZ or BM). The ZF has undergone a growth reaction of the constituents forming this zone. To better interpret the evolution of the fusion line before and after heat treatment at 300 C, magnificated microstructures have been presented (Figure 4). First of all this fusion line has been observed by [15]. As it is shown in, this fusion line is very visible on both sides of the welded joint, and it is a transition line that separates the ZF from the HAZ. The width of this FL can be estimated at 50 µm. This

FL is the preferred site for the onset of solidification of the first solid seeds towards the center of the melting zone. This line disappears after heat treatment at 300 C. This transformation can be attributed to the phenomenon of atomic diffusion across this line and to the rearrangement of the grains adjacent to this line.

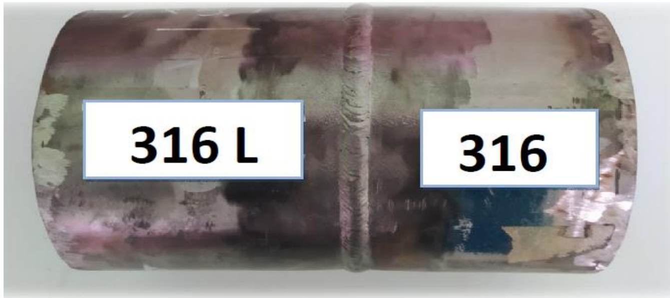

Figure 1**:** *Macrographic view of the welded tubular 316L to 316 austeitic stainless steel (Ø=101 mm, Thickness= 6.02 mm).*

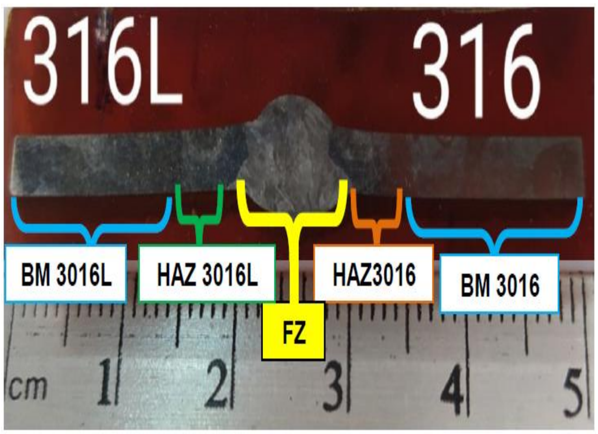

Figure 2: *Macro view of sample taken from 316L to 316 austenitic stainless steel welded tube.*

Table 1: *Chemical composition of 316 and 316L austeitic stainless steels and the electrode.*

	C	Cr	Ni	Mo	Mn	Si	Fe
316	0.08	17.1	10.1	2.0	1.8	0.60	Balance
316L	0.03	17.2	10.4	1.5	1.5	0.60	Balance
ER316L	0.02	19.0	12.5	2.7	1.8	0.55	Balance

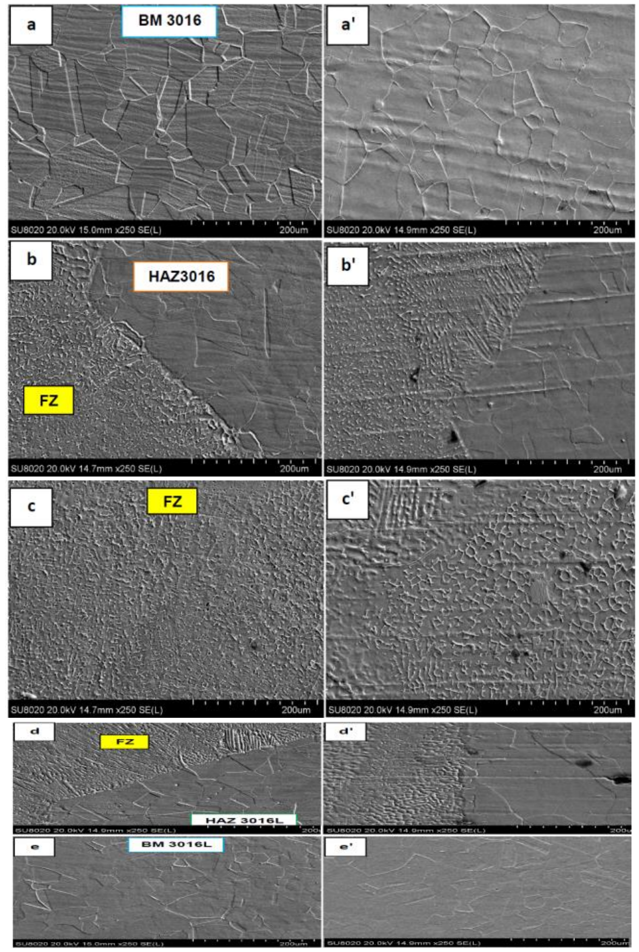

Figure 3 : *Microstructures of welded joint of dissimilar 316L and 316 austenitic stainless steels(a-e), and after heat treatment at 300 °C for 9h (a'-b').*

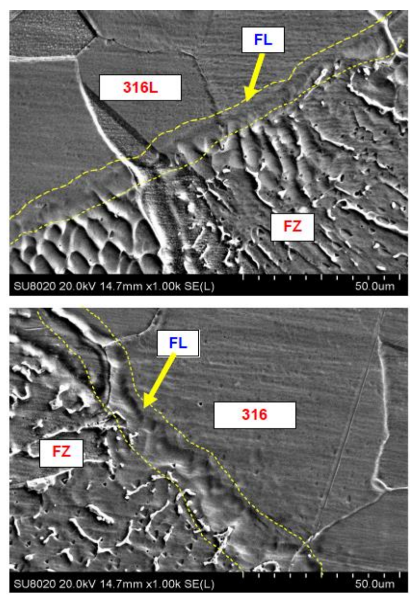

Figure 4: *SEM observations of the two fusion line between fusion zone and a HAZ in welded joint of dissimilar 316L and 316 austenitic stainless steels.*

Citation: Boumerzoug Z, Delaunois F (2022). Effect of Heat Treatment on Dissimilar 316l And 316 Austenitic Stainless Steel TIG Welded Joints. SunText Rev Mat Sci 3(1): 116.

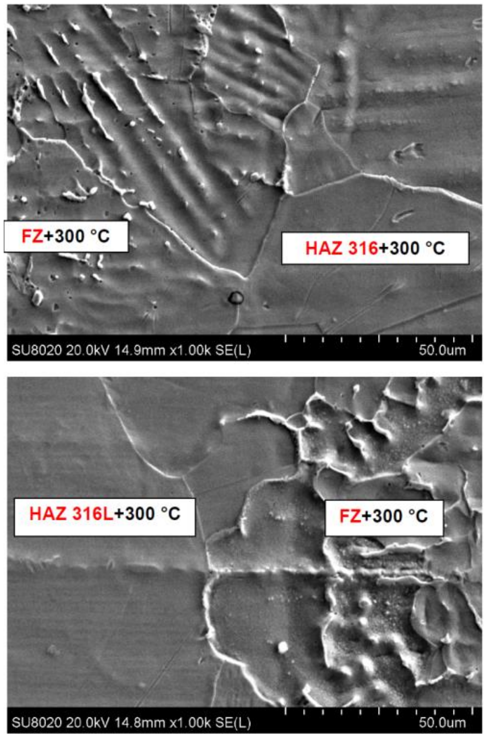

Figure 5: *SEM observations of the two fusion line between fusion zone and a base metal in welded joint of dissimilar 316L and 316 austenitic stainless steels after heat treatment at 300 °C for 9 h.*

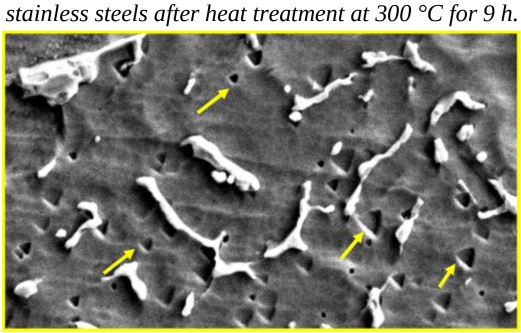

Figure 6: *Magnification of the selected zone in FZ (extracted from Fig.4a) of the welded joint of dissimilar austenitic stainless steels 316L and 316.*

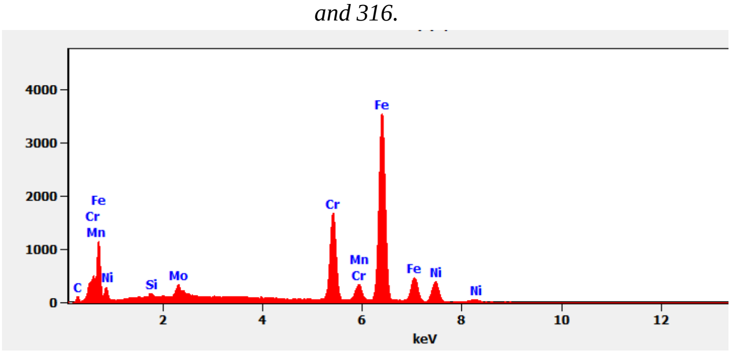

Figure 7: *EDS spectrum of ZF in a welded joint of dissimillar austenitic stainless steels 316L and 316.*

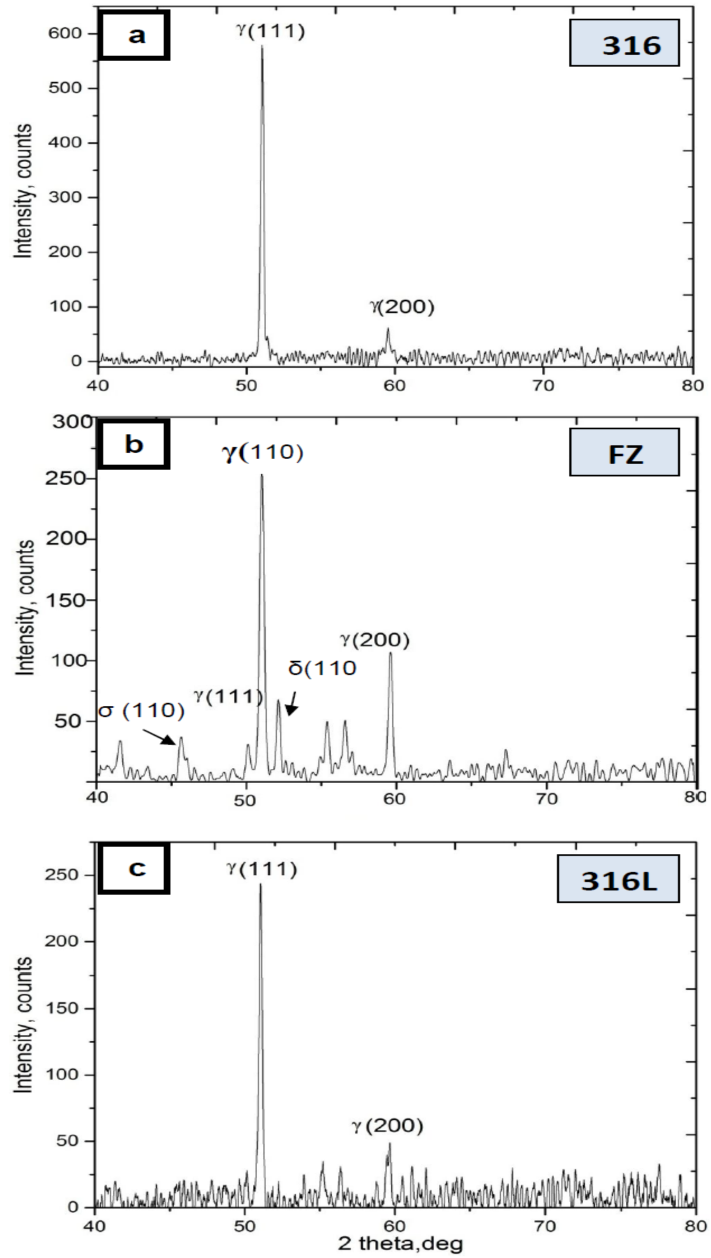

Figure 8: *X-ray diffractograms of fuzion zone (b), base metals 316 (a) and 316L (c) after heat treatment at 300°C for 9h of welded joint of dissimilar austenitic stainless steels 31L6 and 316 .*

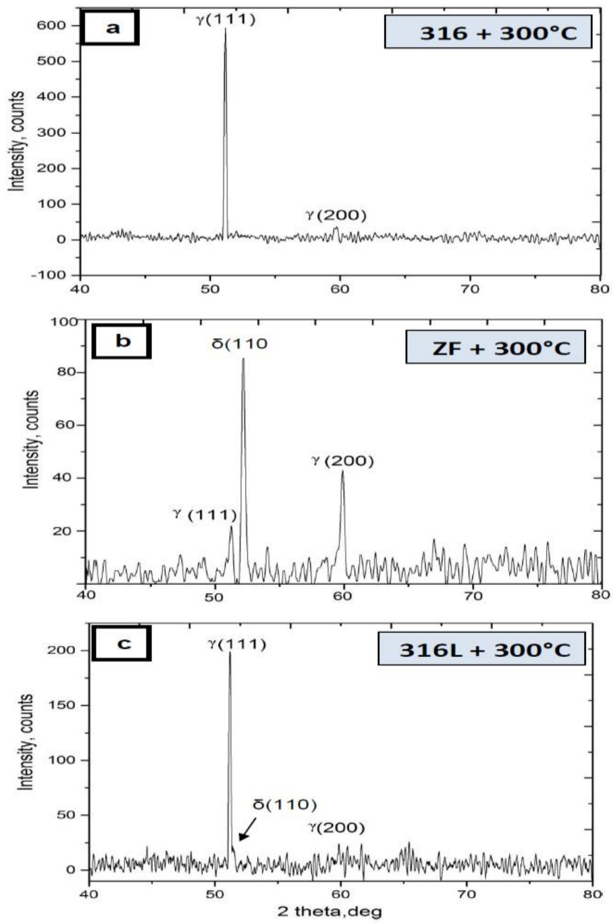

Figure 9 : *X-ray diffractograms of fuzion zone (b), base metals 316 (a) and 316L (c) after heat treatment at 300°C for 9 h of welded joint of dissimilar austenitic stainless steels 316L and 316 .*

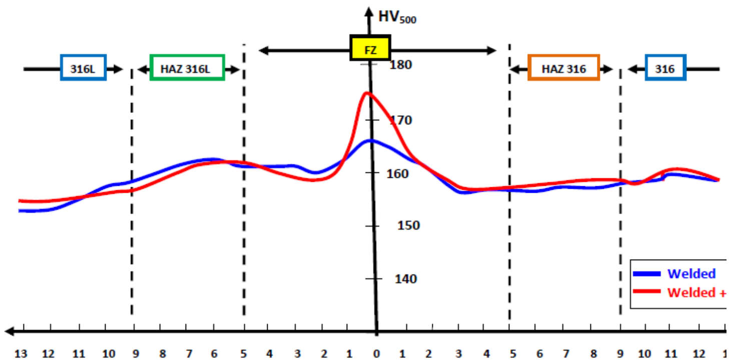

Figure 10: *Profile of hardness variation through the welded joint of dissimilar 316L and 316 austenitic stainless steels, before and after heat treatment at 300°C for 9 h.*

In addition, some etch triangular pits were observed in fusion zone of the welded joint (Figures 5, 6). These pits correspond to the dislocations evoked by many researchers [16-20]. The shape of the etch pits depends on the etching plane. The Etching is sensitive to the crystallographic orientation of the surface. For example, on {111} planes pits are triangular in shape. It has been found that dislocations can be induced by excess of strain during solidification and cooling-down phases investigated the microstructure of dislocations in laser fabricated 316L stainless steel. They found that these high dislocation density zones were Cr-enriched while containing Mn7C3 nanoinclusions [21]. Deep observation of the microstructures of the fusion zone after the heat treatment at 300° C, shows the almost total annihilation of these dislocations, which was an obvious phenomenon. It is known that austenitic steels have an F.C.C atomic structure which provides more planes for the flow of dislocations especially during heat treatments. These results are in agreement with the finding of They found that water-quenched or air-cooled stainless steel solder joints have a relatively high dislocation density. This density decreases with increasing aging temperature after the welding process [22]. The presents the EDS spectrum of chemical analysis in the fusion zone of the welded joint. This result confirms the existence of the main elements (Fe, Cr, Ni, C, Mo, Mn, and Si) which exist in the two dissimilar steels and the electrode (Figure 7).

XRD analysis

The result of the X-ray diffraction analysis of the two zones of the welded joint (two base metals and fusion zone) before and after the heat treatment at 300 C is presented in the (Figures 8,9). The diffractograms of the two base metals before and after heat treatment at 300° C reveal the main austenite peaks without any significant change, except for a change in the intensity of the peaks, which can be attributed either to a slight growth of the grains or to a reorientation of the grains after the heat treatment at 300°C.However, the X-ray diffractogram of the fusion zone before heat treatment (Figure 8) reveals ferrite and austenite peaks with some small peaks. These additional small peaks can be attributed to the precipiatation of carbides or sigma phase. Austenitic stainless steel weld metal has been found to exhibit a duplex microstructure formed from an austenitic matrix containing a dispersion of delta ferrite and the amount of delta ferrite can vary from 3 to 9 %. This ferrite can solve the problem of hot cracking [23,24]. The effect of heat treatment on the fusion zone increased the amount of austenite phase (Figure 9) which is beneficial for the mechanical properties of the welded joint. It has been found that delta ferrite is a metastable phase and can transform upon exposure to high temperature in service or upon heat treatment after welding [25,26].

Hardness Measurements

Shows the hardness variation profile across the weld joint of different 316 and 316L austenitic stainless steels, before and after heat treatment at 300°C for 9 h. For the welded joint and non-heat treated (blue curve) reflects a dissimilar behavior of the joint because the curve on the 316L side is not the same on the 316L

Citation: Boumerzoug Z, Delaunois F (2022). Effect of Heat Treatment on Dissimilar 316l And 316 Austenitic Stainless Steel TIG Welded Joints. SunText Rev Mat Sci 3(1): 116.

side (Figure 10). However, the hardness curve shows a slight high hardness in the fuzion zone (~165Hv). The variation in hardnesses across the weld can be attributed to several factors such as the microstructural difference between the three zones (FZ, HAZ and BM) and the distribution of residual stresses across the weld. Veeresh et al. carried out a numerical study of the residual stresses in the welded joints of the cylindrical shell. They found that the residual stress is maximum near the axis of the weld [27]. It has also been reported that when welding austenitic stainless steels, high residual stresses can be induced in the weld. These stresses come from the low thermal conductivity and the high coefficient of thermal expansion of these steels [28]. However, after the isothermal heat treatment at 300°C (red curve), the hardness of FZ increases and reaches the value of 175 Hv. This is due to the phase transformation in the FZ. In addition, this heat treatment can affect the distribution of residual stresses in the welded joint.

Conclusion

The effect of isothermal heat treatment at 300°C on the microstructure evolution and mechanical properties of welded dissimilar austenitic stainless steels 316L to 316 was studied by scanning electron microscopy, energy dispersive spectroscopy analysis, diffraction X-rays and hardness measurements. The base metal, heat affected zone and fusion zone have been revealed in the welded joint. The fusion zone has a solidifying microstructure with the highest hardness. X-ray diffraction revealed additional phases in the austenitic matrix in the melting zone. In addition, a high dislocation density was observed in the fusion zone which decreases after heat treatment at 300°C. A fusion line is observed between the fusion zone and the heat affected zone, which disappears after heat treatment at 300°C. This heat treatment affected the hardness in the fusion zone than the other zones.

Acknowledgment

We thank Dr. Melik Wafa from the University of Biskra and the PhD student Alexandre Mégret from the University of Mons for their technical assistance.

References

1. Mukahiwa K. Microstructural characterisatiojn of type 316 austenitic stainless steels: implication for corrosion fatigue behavior in PWR primary coolant. PhD Thesis, University of Manchester. 2016.
2. Ezer M, Cam G. Investigation of the microstructure and mechanical properties of gas metal arc welded AISI 304 austenitic stainless steel butt joints. In: Çınar Ö, 2020 Proceedings of International Conference on Eng Tec Innovation (ICETI), 2020; 1-10.
3. Şenol M, Cam G. Microstructural and mechanical characterization of gas metal arc welded AISI 430 ferritic stainless steel joints. In: Çınar Ö, 2020 Proceedings of International Conference on Engineering Technology and Innovation (ICETI). 2020; 1119.
4. Serindağ H, Çam G. Microstructure and mechanical properties of gas metal arc welded AISI 430/AISI 304 dissimilar stainless steels butt joints. 2021.
5. Çam G, Yeni Ç. Erim SInvestigation into properties of laser-welded similar and dissimilar steel joints. Sci Technol Weld Joi, 1998; 3: 177-189.
6. Oyj O. Handbook of Stainless Steel. 2013; 92.
7. Fraser A. Etching 316/316L: How to stain stainless steel. 2022
8. Technical file. 316 vs 316L Stainless Steel: What's the Difference?
9. Kotecki D, Armao F. Welding guide, Stainless steels properties – How to weld them, Where to use them. The Lincoln Electric Company, C6400 publications. 2014; 40.
10. Balaji C, Kumar ASV. Evaluation of mechanical properties of SS 316 L weldments using Tungsten Inert Gas welding .Int J Eng Sci Tec. 2012; 4: 2053-2057.
11. Gowrisankar I, Bhaduri AK, Seetharaman V. Effect of the Number of Passes on the Structure and Properties of Submerged Arc Welds of AISI Type 316L Stainless Steel.Welding Res Suppliment. 1987; 147-15.
12. Singh R, Singh BJ, Singh M. Effect of carbide precipitation on 316L austenitic stainless steel welded joints, Notion Press India.2021; 65.
13. Allahyari AA, Farhangi H. Investigation of aging heat treatment on microstructure and mechanical properties of 316L austenitic stainless steel weld metal. WIT Tra Eng Sci. 2005; 51: 63-72.
14. Dadfar M, Fathi MH, Karimzadeh F, Dadfar MR.Effect of TIG welding on corrosion behavior of 316L stainless steel. Materials Letters. 2007; 61: 2343-2346.
15. Bayock FN, Kah P, Tony KM. Heat input effects on mechanical constraints and microstructural constituents of MAG and laser 316L austenitic stainless-steel welded joints. AIMS Mat Sci. 2022; 9: 236-254.
16. Das GC.Dislocation mobility and plastic deformation in molybdenum single crystals. PhD Thesis, Uni Lon. 1967.
17. Asahi T, Oda O, Taniguchi Y, Koyama A. Characterization of 100 mm diameter CdZnTe single crystals grown by the vertical gradient freezing method. J Cry Gro. 1995; 149: 23-29.
18. Szeles C, Cameron SE, Ndap JO. Advances in the crystal growth of semiinsulating CdZnTe for radiation detector applications. IEEE Tra Nuc Sci. 2002; 49: 2535-254.
19. Mohamed A. Formation and pattern of hexagonal pyramid and triangular etch pits and relationship to dislocation in deformed nickel based super alloys. IOSR J Eng (IOSRJEN). 2013; 3: 53-57.
20. Ivanitska VG, Moravec P, Franc J. Chemical Etching of CdTe in Aqueous Solutions of H2O2-HICitric Acid. J Ele Mat. 2007; 36: 1021-1024.
21. Sprouster DJ, Cunningham WS, Halada GP. Dislocation microstructure and its influence on corrosion behavior in laser additively manufactured 316L stainless steel. Additive Manufacturing. 2021; 47: 102263.
22. Macek K, Luka P, Janove J, Mulka P. Austenite content and dislocation density in electron-beam welds of a stainless maraging steel. Mat Sci Eng. 1996; 208: 131-138.

23. Farrar RA, Huelin C. Phase transformation and impact properties of type 17-8-2 austenitic weld metals, J Mat Sci.1985; 20: 2828-2838.
24. Gill TPS. On microstructure-property correlation of thermally aged type 316L stainless steel weld metal, Met. Trans.1989; 20A: 1115 1124.
25. Shaikh H, Vinoy TV. Correlation of microstructure and tensile properties of 316 stainless steel weld metal solution annealed at high temperatures, Material Science and Technology, 1998;14: 129 -135.
26. Slattery GF. Microstructural transformations in stress relived type 316 stainless steel weld metal. Metallography. 1980; 13: 59-70.
27. Veeresh BR, Suresh R, Gowreesh SS. Numerical investigation of residual stresses in welded joints of cylindrical shell. Metall. Mater. Eng, 2022; 28: 187-202.
28. Smith JJ, Farrar RA. Influence of microstructure and composition on mechanical properties of some AISI 300 series weld metals. Int Mat Rev. 1993; 33: 25-51.